

# Electrical, Thermoelectrical and photo electrochemical properties of $(\text{Sb}_{0.2}\text{Bi}_{0.8})_2\text{S}_3$ Thin films by dip method

S.D.Lakade

Bhausahab Nene College, Pen, Maharashtra. (india)

## Abstract

In the present paper, we have reported the room temperature growth of  $(\text{Sb}_{0.2}\text{Bi}_{0.8})_2\text{S}_3$  thin films by dip method and annealed at various temperatures. The films were deposited from a reaction bath containing antimony chloride, glycine and sodium thiosulphate. We have analyzed the electrical, thermoelectrical and photoelectrochemical properties of thin films. The conductance of the samples is  $1.021 \times 10^{-6} (\Omega \text{ cm})^{-1}$ . The specific conductance will increase for pseudo-binary films with annealing temperature. Thermoelectric power increases from 283.43 to 327.28  $\mu\text{V}/\text{K}$  as the temperature increases from 300 to 525 K. open circuit voltage and short-circuit current is obtained to be 284 mV and 2.42  $\text{mA}/\text{cm}^2$  correspondingly for photoelectrode annealed at 473 K. The calculations indicate that the fill parameter is 38.51% and solar energy exchange output is 0.148% for sample annealed at 473 K. At 473 K have relative optical energy consequences in improvement in power output.

**Keywords:**  $(\text{Sb}_{0.2}\text{Bi}_{0.8})_2\text{S}_3$ , Thin film, electrical, thermo electrical, photoelectrochemical.

## Introduction

The electronic and optical properties of binary and ternary semiconductor materials of group VI have been extensively studied due to their important nonlinear, luminescent properties, Quantum size effect [1,2]. Polycrystalline electrodes of compounds with large area are economically desirable for solar cell applications. Semiconductor liquid junction solar cells have been attracting attention in the last few years, due to growing interest in solar energy conversion [3]. These cells are simple in construction and have an advantage that they can be used for both photo voltage and chemical energy conversion. In the field of energy conversion, semiconductor electrolyte interface may be used for photoelectrolysis, photo catalysis and photoelectrochemical power generation.  $\text{Bi}_2\text{Se}_3$  and  $\text{Sb}_2\text{Se}_3$  compounds are the members of V-VI group of materials. The band gap of single-crystal  $\text{Bi}_2\text{Se}_3$  was reported earlier as eg. 0.35 eV [4] which lies in the infrared region (within the wavelength range 850-2000 nm). To make it the visible region (within wavelength range of 350-850 nm) of solar spectrum, another compound like  $\text{Sb}_2\text{Se}_3$  whose band gap  $E_g = 1.88$  eV [5] is mixed with  $\text{Bi}_2\text{Se}_3$  so that combination of two gives better result in application such as photosensitivity and photoconductivity [6-8]. Similarly, some reports are available for the deposition of  $\text{CdS}-\text{Cu}_x\text{S}$  [9],  $\text{PbS}-\text{Cu}_x\text{S}$  [10], and  $\text{Bi}_2\text{S}_3-\text{Cu}_x\text{S}$  [11] and have illustrated or suggested their applications in the area of energy conversion and solar energy utilization [12] due to modification in electrical and optical properties

Different workers have reported chemical deposition of  $\text{Bi}_2\text{S}_3$  on different types of substrates with characterization such as chemical deposition [13], interface gas–solution [14], electrodeposition [15], and spray pyrolysis [16]. Krishnamurthy and Shivkumar [17] deposited  $\text{Bi}_2\text{S}_3$  films using the hot wall chemical deposition technique. Benramdane et al. [18] deposited  $\text{Bi}_2\text{S}_3$  films onto glass substrates by spray pyrolysis method using bismuth chloride and thiourea having bismuth and sulphur source respectively. Pawar et al. [19,20] prepared amorphous  $\text{Bi}_2\text{S}_3$  and  $\text{Sb}_{2-x}\text{Bi}_x\text{S}_3$  films by the solution–gas interface method. Electrodeposition method was used by Lokhande and Bhosale [21] to prepare polycrystalline  $\text{Bi}_2\text{S}_3$  thin films. Krishna Moorthy [22] has prepared polycrystalline stoichiometric  $\text{Bi}_2\text{S}_3$  films by physical deposition technique. Pramanik and Bhattacharya [23] have also deposited amorphous  $\text{Bi}_2\text{S}_3$  thin films from an alkaline bath using TEA as a complexing agent. Biswas et al. [24] have prepared thin films of  $\text{Bi}_2\text{S}_3$  by solution growth technique using triethanolamine (TEA) as the complexing agent. Lokhande et al. [25,13] have deposited thin films of  $\text{Bi}_2\text{S}_3$  from an alkaline as well as acidic bath using EDTA complexing agent. Ubale et al. [26] have prepared  $\text{Bi}_2\text{S}_3$  thin films by modified chemical bath deposition at room temperature and reported their electrical and optical properties. The non-aqueous chemical deposition of the  $\text{Bi}_2\text{S}_3$  thin films has been reported by Desai and Lokhande [27] using bismuth nitrate and thiourea in acetic acid and formaldehyde solvents respectively.

In the present investigation,  $(\text{Sb}_{0.2}\text{Bi}_{0.8})_2\text{S}_3$  multilayer thin film deposited by simple chemical bath deposition method were used at room temperature. The deposited samples are characterized by electrical, thermo electrical and photoelectrochemical properties are also studied.

## 2: Experimental Details

### Deposition of $(\text{Sb}_{0.2}\text{Bi}_{0.8})_2\text{S}_3$ Thin Films

The deposition of typical  $(\text{Sb}_{0.2}\text{Bi}_{0.8})_2\text{S}_3$  thin films samples was synthesized from a reaction mixture. The chemical substances have been used in the following manner: 8 mL (0.2M) Bismuth nitrate, 2 mL (0.2M) Antimony trichloride, 4 mL (1M) Glycine and 15 mL (0.2M) sodium thiosulphate was mixed in each bath. The overall quantity of the prepared solution to 50 mL by using double distilled water. The bath consists of reaction mixture became kept in ice bath at temperature 278 K. The pH of reactive mixture became observed 4.86. Glass slides as well as stainless steel strips were maintained vertically to some extent slanted in a reaction mixture. The temperature of the reactive mixture became permissible to increase very gradually to 298 K. The glass slides and stainless steel material were removed from the bath after four hour. When the deposition process completed, the substrates have been eliminated from the reactive mixture, rinsed with the help of distilled water. The samples were dried in atmosphere. The sample was deposited on both sides of glass and stainless steel materials. The films were annealed at 348K, 423K and 473K for 3 hours.

## 3: Result and Discussions:

### 3.1: Electrical Characterization of $(\text{Sb}_{0.2}\text{Bi}_{0.8})_2\text{S}_3$

The electrical conductance of  $(\text{Sb}_{0.2}\text{Bi}_{0.8})_2\text{S}_3$  samples on amorphous substrates became measured. At normal temperature the specific conductivity became observed in the range of  $10^{-6}(\Omega\text{cm})^{-1}$ . The small value of

conductivity for samples was observed. This is because of some amorphous nature and minute thickness of the thin samples. The electrical characteristics of crystalline samples are mostly relying on their crystallographic properties and elemental analysis. A graph of  $\log(\text{conductivity})$  against inverse absolute temperature is represented in diagram: 1. a graph indicates two areas, the smaller temperature extrinsic area and higher temperature intrinsic area, confirming the occurrence of two type electrical conduction process. The higher temperature area was mainly because of grain border scattering limited conduction process, whereas a small temperature area is because of variable range hopping conduction process. The activation energy is determined applying Arrhenius relation.

In the current study the activation energies have been in the limit of 0.108-0.208 eV. The small value of activation energies suggests the presence of an imperfection level under the conduction or over the valence band. The magnitude of activation energy reliable with formerly determined. As the thermal activation energy indicates a mean magnitude of the barrier height between two adjacent crystals. It is a combining consequence of carrier density and mobility. It is predictable that observed magnitude of activation energy will be different among researcher usage of diverse deposition situations. Though, the common reliance of conductance on temperature is obviously steady, and shows the presence of a distinct potential barrier among grains of adjacent crystals; that can be conquer with the aid of thermal activation. As the temperature rise, the conductance is found out raise to some extent at beginning and following reaching approximately 357 K, it will increase constantly. The conductance of the  $(\text{Sb}_{0.2}\text{Bi}_{0.8})_2\text{S}_3$  samples is  $1.021 \times 10^{-6} (\Omega \text{ cm})^{-1}$  ( $T = 300 \text{ K}$ ) and  $1.029 \times 10^{-3} (\Omega \text{ cm})^{-1}$  ( $T = 525 \text{ K}$ ). Granule junction discontinuity and thickness of the samples can be dependable for lower conductance of the  $(\text{Sb}_{0.2}\text{Bi}_{0.8})_2\text{S}_3$  films.

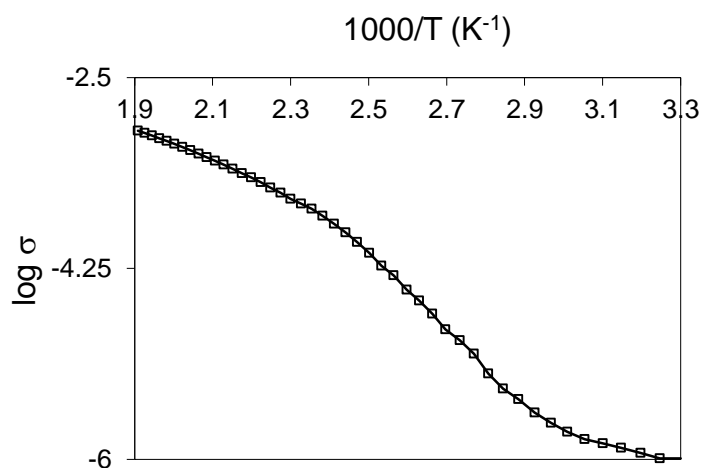


Diagram 1: Plot of conductivity in opposition to inverse of absolute temperature of  $(\text{Sb}_{0.2}\text{Bi}_{0.8})_2\text{S}_3$  thin film

### 3.2: Electrical Characterization of Annealed $(\text{Sb}_{0.2}\text{Bi}_{0.8})_2\text{S}_3$ Thin Films

The dark electrical conductivity of annealed  $(\text{Sb}_{0.2}\text{Bi}_{0.8})_2\text{S}_3$  film on non-conducting glass slide was determined by using a 'dc' two probe method, in the temperature range 300-525K. The conductance of the thin films will rise with raise in temperature, indicative of semiconducting nature of the sample. The value of

electrical conductivity for sample 348 K was found to be 0.9 nA at 300K while 0.834  $\mu\text{A}$  at 525K. Similarly, the value of electrical conductivity for sample annealed at 473 K was found to be 1.1 nA at 300K while 0.902  $\mu\text{A}$  at 525K. The low value of conductivity for the film may be due to low crystallinity and small thickness of the film. A common rise in the electrical conductance can be because of reduction in the optical energy of the samples and rise in particle dimension having raise in the annealing temperature. The particle dimension raise as intern clear area decreases and reduces the height of granule junction potential ensuing in increases in the carrier density in addition to the carrier mobility and for that reason electrical conductance. The value of specific conductance was found to be  $1.186 \times 10^{-6} (\Omega \text{ cm})^{-1}$  at 300K and  $1.54 \times 10^{-3} (\Omega \text{ cm})^{-1}$  at 525 K for sample annealed at 348 K. Similarly, specific conductance was found to be  $1.704 \times 10^{-6} (\Omega \text{ cm})^{-1}$  at 300 K and  $2.11 \times 10^{-3} (\Omega \text{ cm})^{-1}$  at 525 K for sample annealed at 473 K. The specific conductance will increases for pseudo-binary films with annealing temperature. The graphs of log conductivity against inverse of temperature are represented in diagram 2 (a-c) for annealed  $(\text{Sb}_{0.2}\text{Bi}_{0.8})_2\text{S}_3$  thin samples. It contains two separate areas, confirming the occurrence of two- type conduction method, the small temperature intrinsic and high temperature extrinsic. In the smaller temperature area (300-370 K) is represented via low magnitude of slope. Above this temperature, the curve is characterized by larger slope. The activation energy is estimated usage of expression.

$$\sigma = \sigma_0 \exp (-E_a/KT) \text{ -----[1]}$$

The thermal activation energies determined using the slope of linear portion of log conductivity against inverse of temperature graph. The activation energies for different low temperature region were found between 0.102 to 0.089 eV. While, for high temperature region activation energies were observed between 0.201 to 0.183 eV. The activation energy found randomly varies with the annealing temperature.

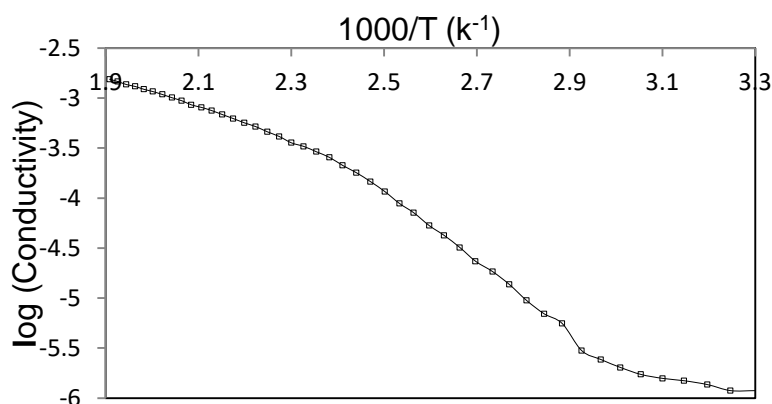


Diagram 2 (a): Plot of conductivity in opposition to inverse of absolute temperature of annealed  $(\text{Sb}_{0.2}\text{Bi}_{0.8})_2\text{S}_3$  thin film at 348 K

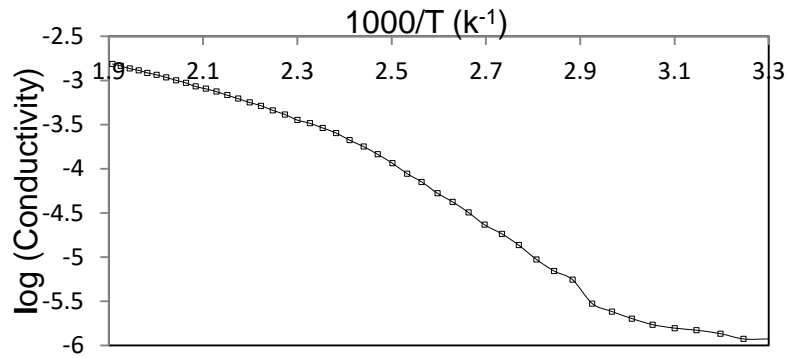


Diagram 2 (b): Plot of conductivity in opposition to inverse of absolute temperature of annealed  $(\text{Sb}_{0.2}\text{Bi}_{0.8})_2\text{S}_3$  thin film at 423 K

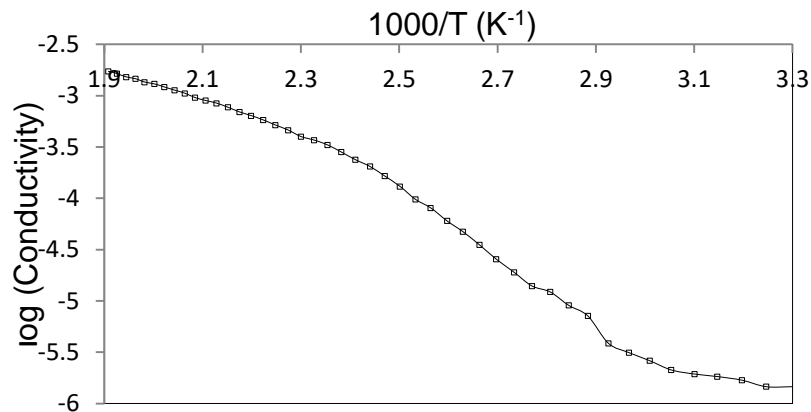


Diagram: 2 (c): Plot of conductivity in opposition to inverse of absolute temperature of annealed  $(\text{Sb}_{0.2}\text{Bi}_{0.8})_2\text{S}_3$  thin film at 473K

### 3.3: Thermoelectrical Characterization of $(\text{Sb}_{0.2}\text{Bi}_{0.8})_2\text{S}_3$ Sample

Thermoelectrical power determination of  $(\text{Sb}_{0.2}\text{Bi}_{0.8})_2\text{S}_3$  samples indicates raise in thermoelectric power with rising temperature. The raise in thermoelectric power by temperature confirms the uniform nature of the samples. The polarity of thermo electromotive force was positive related hot end w.r.t. cold end that indicates that  $(\text{Sb}_{0.2}\text{Bi}_{0.8})_2\text{S}_3$  samples shows n-kind conductance. The temperature reliance of thermoelectric power is represented in diagram: 3. The thermoelectric power is nearly straight at low temperature areas, wherein because it differs at high temperature. Thermoelectric power was increases from 283.43 to 327.28  $\mu\text{V}/\text{K}$  as the temperature increases from 300 to 525 K. Carrier concentration can be calculated using equation <sup>28</sup>

$$\log n = 3/2 \log T - 0.005 P + 15.7198 \text{-----} [2]$$

The carrier concentration (n) has been calculated in the range of 300 to 525 K. At 300 K, the carrier density became observed to be  $1.058 \times 10^{18}$ . Carrier concentration increases as the temperature raise. The equation

$$\mu = \sigma/ne \text{-----} [3]$$

Was applied to calculate the carrier mobility. It was observed to be  $6.026 \times 10^{-6}$  at 300 K and  $4.432 \times 10^{-3}$  at 525 K. The electrical conductance rise with raise in temperature due to increase in carrier concentration and



carrier mobility, which confirms semiconducting character of the sample. The grain boundary potential was calculated by using equation

$$\mu = \mu_0 \exp (-\Phi_B / KT) \text{-----}[4]$$

The grain boundary potential is calculated by using a graph of  $\log \mu T^{1/2}$  versus  $1000/T$ . The magnitude of  $\Phi_B$  became estimated to be 0.462 eV.

### 3.4: Thermoelectrical Characterization of Annealed $(\text{Sb}_{0.2}\text{Bi}_{0.8})_2\text{S}_3$ Thin Films

Thermoelectric power measured for annealed  $(\text{Sb}_{0.2}\text{Bi}_{0.8})_2\text{S}_3$  films in the range of 300-525K. This shows rising thermoelectric power with rising temperature for all the films. This indicates degenerate character of the samples. The sign of thermo- electromotive force became positive to hot end w r. t. cold end, that suggests annealed  $(\text{Sb}_{0.2}\text{Bi}_{0.8})_2\text{S}_3$  samples shows n-kind conductivity. The temperature reliance of thermoelectric power was represented in diagram:

4 (a-c). The thermoelectric power is more or less linear in small temperature area, while it varies abruptly at high temperature. As the annealing temperature increases, linearity goes increases. Thermoelectric power was found to be 286.64 to 330.64  $\mu\text{V}/\text{K}$  in the temperature range from 300-525 K for sample annealed at 348 K. For sample annealed at 473 K, thermoelectric power changes from 293.54 to 340.53  $\mu\text{V}/\text{K}$  as the temperature increase from 300 to 525K. This indicates as the annealing temperature increases the thermoelectric power increases. The linear nature of the graph was observed. The carrier concentration with respect to temperature is calculated using equation

$$\log n = 3/2 \log T - 0.005 P + 15.7198 \text{-----}[5]$$

For the entire sample. At 300 K, the carrier density became observed to be  $1.084 \times 10^{18}$  and  $1.461 \times 10^{18}$  at 525 K for sample annealed at 348 K. For other extreme i.e. annealing temperature 473 K, the value of carrier concentration was found to be  $1.096 \times 10^{18}$  at 300 K and  $1.479 \times 10^{18}$  at 525 K. As the annealing temperature rise the carrier concentration increases.

Carrier concentration increases as the temperature rise. At low temperature the value of carrier concentration is low, but higher temperature carrier concentration increases. The relation

$$\mu = \sigma / ne \text{-----}[6]$$

Was applied to calculate the carrier mobility of all the samples. For sample annealed at 348 K, carrier mobility was found to be  $5.834 \times 10^{-6}$  at 300 K and  $2.953 \times 10^{-3}$  at 525 K. For sample annealed at 473K, carrier mobility was found to be  $5.446 \times 10^{-6}$  at 300 K and  $1.484 \times 10^{-3}$  at 525 K. It was found that carrier mobility rise with raise in temperature. In temperature range 300- 375K the change in carrier mobility is very less. But afterwards, it increases steeply. Both graph shows same nature. The grain boundary potential became calculated by using a graph of  $\log \mu T^{1/2}$  with inverse temperature. The magnitude of  $\Phi_B$  became observed to be decreases from 0.441 to 0.425 eV as the annealing temperature increases.

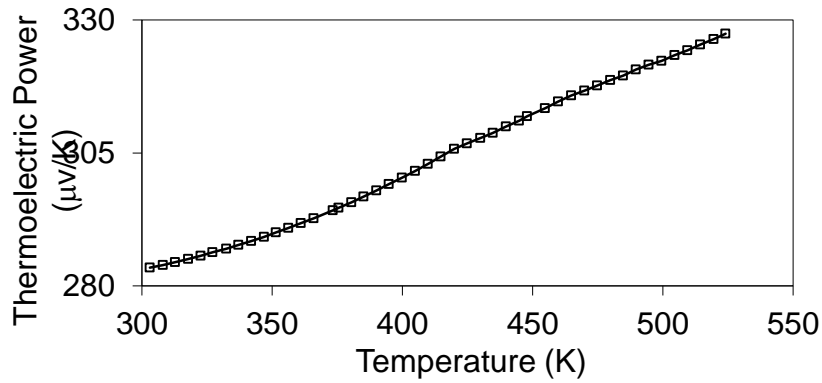


Diagram 3-: Thermoelectric power measurement of  $(Sb_{0.2}Bi_{0.8})_2S_3$  thin film

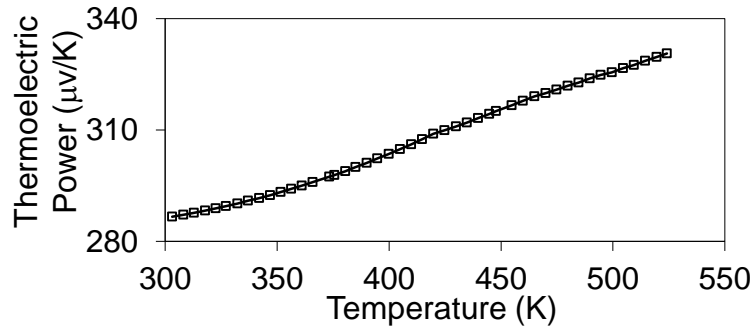


Diagram 4 (a)-: Thermoelectric power measurement of annealed  $(Sb_{0.2}Bi_{0.8})_2S_3$  at 348 K

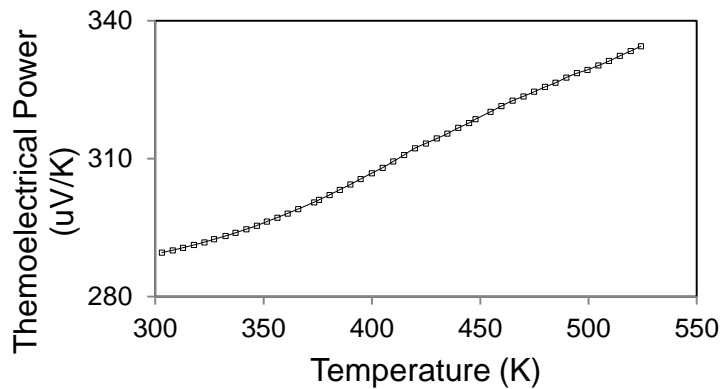


Diagram 4 (b)-: Thermoelectric power measurement of annealed  $(Sb_{0.2}Bi_{0.8})_2S_3$  thin film at 423 K

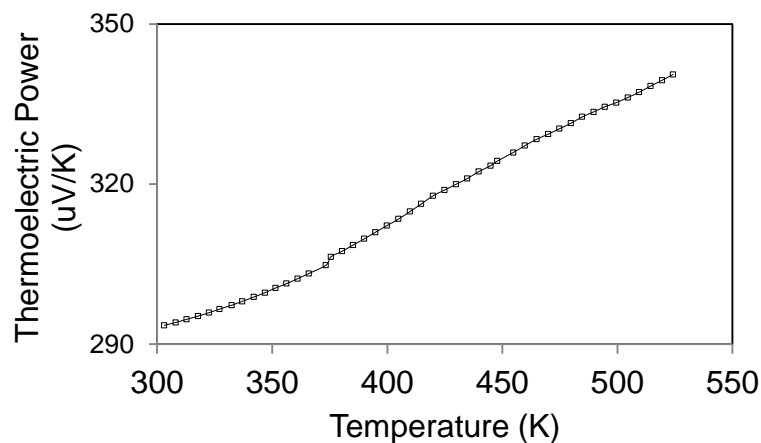


Diagram 4 (c)-: Thermoelectric power measurement of annealed  $(\text{Sb}_{0.2}\text{Bi}_{0.8})_2\text{S}_3$  at 473 K

### 3.5: Photoelectrochemical Analysis

Current-voltage characteristics and power output characteristics of  $(\text{Sb}_{0.2}\text{Bi}_{0.8})_2\text{S}_3$  and annealed  $(\text{Sb}_{0.2}\text{Bi}_{0.8})_2\text{S}_3$  photoelectrode were tested.

### 3.6: Contact

An ohmic contact is necessary between deposited photoelectrode and the substrate. It is non-injecting and has a linear current-voltage relation in both directions. The nature of contact of the semiconductor photoelectrode and stainless steel plate was checked for all samples. Current-voltage relations were found to be straight line in both directions, suggesting the ohmic behavior of contact.

### 3.7: Conductivity Type

A photoelectrochemical cell with design  $n\text{-}(\text{Sb}_{0.2}\text{Bi}_{0.8})_2\text{S}_3 \mid \text{NaOH (1M)} + \text{S (1M)} + \text{Na}_2\text{S (1M)} \mid \text{C (graphite)}$  was fabricated. Dark voltage and dark current was observed in the dark. The sign of dark potential difference became negative related to semiconducting photoelectrode. The indication of the photo voltage suggests the conductivity nature of  $(\text{Sb}_{0.2}\text{Bi}_{0.8})_2\text{S}_3$  and annealed  $(\text{Sb}_{0.2}\text{Bi}_{0.8})_2\text{S}_3$ . This proves that all the samples are an n-kind semiconductor that has also been confirmed from thermoelectric determination.

### 3.8: Current-voltage Properties in Dark

These properties of  $(\text{Sb}_{0.2}\text{Bi}_{0.8})_2\text{S}_3$  and annealed  $(\text{Sb}_{0.2}\text{Bi}_{0.8})_2\text{S}_3$  photoelectrochemical cell in dark were examined at room temperature and represented in diagram:5. The rectifying type of junction was confirmed by the non-symmetrical nature of the graph. Existence of some dark current shows that there is some worsening of the photoelectrode samples in the solution. Taking into grantable photoelectrode-electrolyte junction as the analog of a Schottky barrier cell, the current transfer throughout the junction is known by a Bulter-Volmer relation. The features are non-symmetrical suggesting the development of rectifying nature junction. In the current analysis,  $\beta$  factor became observed to be more than 0.5 for the entire samples indicating the rectifying character of the junction. The junction ideality consideration may be measured applying the plot of  $\log I$  in opposition to potential difference and the variant is represented in diagram: 6. linear character of the graph became applied



for the determination of ideality parameters. The calculated ideality factor became observed to be 2.10 for  $(\text{Sb}_{0.2}\text{Bi}_{0.8})_2\text{S}_3$  thin films. Sample annealed at 348 K gave 1.99 junction ideality factor. As the annealing temperature increases the junction ideality factor decreases. The larger value of junction ideality factor shows the domination of series resistance in addition to structural defect induced via variation in the antimony and bismuth ionic dimension and their ensuing array in the solid throughout lattice building. It additionally indicates that average transfer in between the semiconductor electrolyte interface with important involvement from surface states and deep traps. It was found to be minimum for photoelectrode annealed at 473K and found to be 1.83. Imperfection levels were inserted in this manner within the valance and optical gap works as carrier traps or combination point. The value of junction ideality parameter was found a least for photoelectrode annealed at 473 K signifying smallest trap density at the semiconductor photoelectrode electrolyte junction.

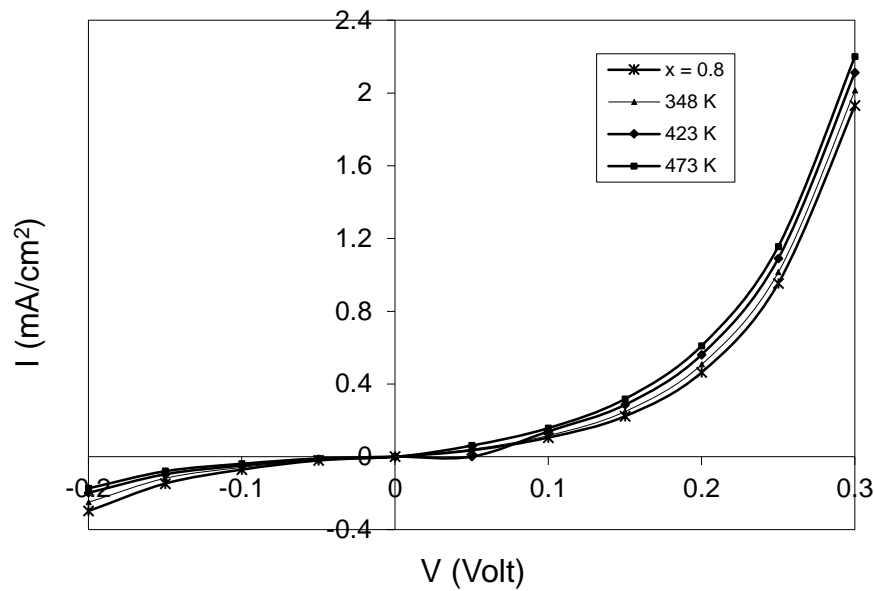


Diagram 5: I-V characteristics of annealed  $\text{Sb}_{0.2}\text{Bi}_{0.8}\text{S}_3$  photoelectrode

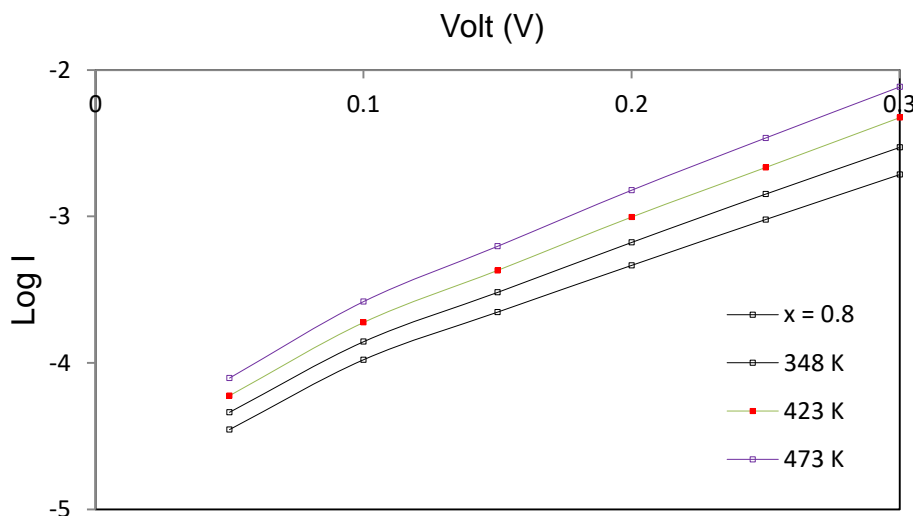


Diagram 6: Plot of  $\log I$  with Voltage of annealed  $(\text{Sb}_{0.2}\text{Bi}_{0.8})_2\text{S}_3$  cells.

### 3.9: Power Output Properties

The photoelectrochemical cell power putout properties for a fabricated cell under light intensity of 30 mW/cm<sup>2</sup> The variety of cell parameters such as output efficiency ( $\eta$ ), open circuit voltage ( $V_{oc}$ ), series resistance ( $R_s$ ), fill factor (ff), shunt resistance ( $R_{sh}$ ), short-circuit current ( $I_{sc}$ ), became measured for  $(Sb_{0.2}Bi_{0.8})_2S_3$  and annealed  $(Sb_{0.2}Bi_{0.8})_2S_3$  the photoelectrodes.

### 3.10: Power Output Characteristics of $(Sb_{0.2}Bi_{0.8})_2S_3$ Photoelectrode

Diagram: 7 shows power output characteristics for  $(Sb_{0.2}Bi_{0.8})_2S_3$  thin films. Ideal photovoltaic power curves should be a quadrangle giving nil series resistance and infinite shunt resistance. In the present investigation, these curves show deviation from ideal behavior at smaller thickness. This is because of the large series resistance and finite magnitude of shunt resistance of the cell. The highest power production of the device is determined with the aid of the biggest rectangle which may be drawn in the arc. The open circuit voltage and short circuit current have been observed to be 250 mV and 1.93mA/cm<sup>2</sup> correspondingly. The calculations lead to fill parameter 37.30% and power output conversion efficiency 0.12%. The series and shunt resistance have been estimated using the slopes of power output properties applying the equation

$$(dI/dV)_{I=0} = (1/R_s) \text{-----}[7]$$

$$(dI/dV)_{V=0} = (1/R_{sh}) \text{-----}[8]$$

The series and shunt resistance became calculated to be 198  $\Omega$  and 617  $\Omega$  correspondingly. The smaller competence can be because of higher shunt resistance and boundary states that are accountable for combination method.

### 3.11: Power Output Characteristics of Annealed $(Sb_{0.2}Bi_{0.8})_2S_3$ Photoelectrode

Diagram: 7 indicates the photoelectrochemical power production properties of different cells have been studied under light. Short-circuit current, open circuit voltage, fill parameter and energy output raise as the annealing temperature increases. The series and shunt resistance get reduced as the annealing temperature increases. The open circuit voltage and short-circuit current is obtained to be 260mV and 2.14 mA/cm<sup>2</sup> correspondingly for photoelectrode annealed at 348 K. The calculations indicate that the fill parameter is 37.68% and solar energy exchange output is 0.127% for sample annealed at 348 K.

Similarly, open circuit voltage and short-circuit current is obtained to be 284 mV and 2.42 mA/cm<sup>2</sup> correspondingly for photoelectrode annealed at 473 K. The calculations indicate that the fill parameter is 38.51% and solar energy exchange output is 0.148% for sample annealed at 473 K. At 473 K have relative optical energy consequences in improvement in power output. The higher short circuit current because of lowered sample resistance and improved the light absorption via the sample. The low competence in the current research may be because of the higher series resistance of the photoelectrochemical device, lower thickness of the sample and junction states that are responsible for the combination phenomenon. The series and shunt resistance have been determined for all the samples. The values of series and shunt resistance have been

observed to be 184 and 597  $\Omega$  correspondingly for sample annealed at 348 K. The values of series and shunt resistance have been observed to be 153 and 567  $\Omega$  correspondingly for sample annealed at 473 K.

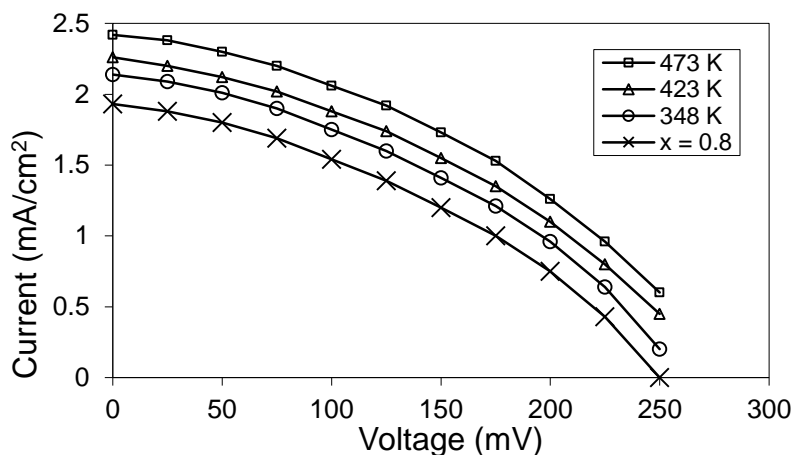


Diagram: 7 Photovoltaic output characteristics for annealed  $(\text{Sb}_{0.2}\text{Bi}_{0.8})_2\text{S}_3$  photoelectrode using polysulphide electrolyte.

### Conclusion:

- 1) The conductance of the  $(\text{Sb}_{0.2}\text{Bi}_{0.8})_2\text{S}_3$  samples is  $1.021 \times 10^{-6} (\Omega \text{ cm})^{-1}$  ( $T = 300 \text{ K}$ ) and  $1.029 \times 10^{-3} (\Omega \text{ cm})^{-1}$  ( $T = 525 \text{ K}$ ). Granule junction discontinuity and thickness of the samples can be dependable for lower conductance of the films.
- 2) The specific conductance will increase for pseudo-binary films with annealing temperature.
- 3) It was found that carrier mobility rises with an increase in temperature.
- 4) The series and shunt resistance have been determined for all the samples. The values of series and shunt resistance have been observed to be 184 and 597  $\Omega$  correspondingly for sample annealed at 348 K. The values of series and shunt resistance have been observed to be 153 and 567  $\Omega$  correspondingly for sample annealed at 473 K.

### Acknowledgement:

The author is thankful to Dr.P.A. Chate for encouragement and support. our sincere thank to chemistry faculty. Thanks to chemistry laboratory staff for cooperation during research work. I would also like to express my gratitude to Miss. Kajal Subhash lakade for helping me in the research work.

### References

- [1] J.-C. Jan, Shou-Yi-Kuo, S.-B. Yin, W.-F. Hsieh, *Chines J. Phys.* 39, 90 (2001)
- [2] R.B. Kale, S.D. Sartale, B.K. Chougale, C.D. Lokhande, *Semicond. Sci. Tech.* 19, 980 (2004)
- [3] H. Minourca, M. Tsuiki, T. Oki, Busenges, *Phys. Chem.* 81 (1997) 588.
- [4] J.C. Bailar Jr., J. Urbanan, H.J. Emeleus, T.F. Trotman-Dickenson, *Comprehensive Inorganic Chemistry*, Vol. 2, Pergamon Press, Oxford, 1973, p. 616.
- [5] P. Pramanik, R.N. Bhattacharya, *Solid State Commun.* 44 (1982) 425.

- [6] J.S. Curran, R. Phillipe, Proceedings of the 14th International Conference on ECPV Solar Energy, Stressa, 10}14, May, 1982. *B.R. Sankapal, C.D. Lokhande / Solar Energy Materials & Solar Cells 69 (2001) 43}52 51*
- [7] G. Ghosh, B.P. Varma, *Solid State Commun.* 31 (1979) 683.
- [8] G. Ghosh, B.P. Varma, *Thin Solid Films* 60 (1979) 61.
- [9] P.K. Nair, M.T.S. Nair, J. Campos, *Proc. SPIE* 823 (1987) 256.
- [10] P.K. Nair, M.T.S. Nair, *Semicond. Sci. Technol.* 4 (1989) 807.
- [11] P.K. Nair, M.T.S. Nair, *Semicond. Sci. Technol.* 7 (1992) 239.
- [12] P.K. Nair, M.T.S. Nair, A. Fernandez, M. Ocampo, *J. Phys. D* 22 (1989) 829.
- [13] C.D. Lokhande, A.U. Ubale, P.S. Patil, *Thin Solid Films* 302 (1997) 1.
- [14] S.H. Pawar, P.N. Bhosale, M.D. Uplane, S. Tamhankar, *Thin Solid Films* 110 (1983)165.
- [15] N.S. Yesugade, C.D. Lokhande, C.H. Bhosale, *Thin Solid Films* 263 (1995) 145.
- [16] V.V. Killedar, C.D. Lokhande, C.H. Bhosale, *Thin Solid Films* 289 (1996) 14.
- [17] P.A. Krishnamurthy, G.K. Shivkumar, *Thin Solid Films* 121 (1984) 151.
- [18] N. Benramdane, M. Latreche, H. Tabet, M. Boukhalfa, Z. Kebbab, A. Bouzidi, *Mater. Sci. Eng. B* 64 (1999) 84.
- [19] S.H. Pawar, P.N. Bhosale, *Bull. Electrochem. I* (1985) 495.
- [20] S.H. Pawar, P.N. Bhosale, M.D. Uplane, S.P. Tamhankar, *Thin Solid Films* 110(1983) 165.
- [21] C.D. Lokhande, C.H. Bhosale, *Bull. Electrochem.* 6 (1990) 622.
- [22] P.A. Krishna Moorthy, *J. Mater. Sci. Lett.* 3 (1984) 551.
- [23] P. Pramanik, R.N. Bhattacharya, *J. Electrochem. Soc.* 127 (1980) 2087.
- [24] S. Biswas, A. Mondal, D. Mukherjee, P. Pramanik, *J. Electrochem. Soc.* 133 (1) (1986) 48.
- [25] C.D. Lokhande, V.S. Yermune, S.H. Pawar, *J. Electrochem. Soc.* 135 (1988)1852.
- [26] A.U. Ubale, A.S. Daryapurkar, R.B. Mankar, R.R. Raut, V.S. Sangawar, C.H. Bhosale, *Mater. Chem. Phys.* 110 (2008) 180.
- [27] J.D. Desai, C.D. Lokhande, *Mater. Chem. Phys.* 34 (1993) 313.
- [28] Mankarious R. (1964) Hall mobility measurements on CdS films. *Solid State Electron.* 7: 702-704.